A broad-host-range CRISPRi toolkit for silencing gene expression in Burkholderia

Short Title: CRISPRi toolkit for Burkholderia

Andrew M. Hogan[1], A. S. M. Zisanur Rahman[1], Tasia J. Lightly[1], Silvia T. Cardona[1,2*].

[1]Department of Microbiology, University of Manitoba, Winnipeg, MB, Canada.

[2]Department of Medical Microbiology & Infectious Disease, University of Manitoba, Winnipeg, Canada.

*To whom correspondence should be addressed: Silvia.Cardona@umanitoba.ca

Abstract

Genetic tools are critical to dissecting the mechanisms governing cellular processes, from fundamental physiology to pathogenesis. Members of the genus *Burkholderia* have potential for biotechnological applications but can also cause disease in humans with a debilitated immune system. The lack of suitable genetic tools to edit *Burkholderia* GC-rich genomes has hampered the exploration of useful capacities and the understanding of pathogenic features. To address this, we have developed CRISPR interference (CRISPRi) technology for gene silencing in *Burkholderia*. Tunable expression was provided by placing a codon-optimized *dcas9* from *Streptococcus pyogenes* under control of a rhamnose-inducible promoter. As a proof of concept, the *paaABCDE* operon controlling genes necessary for phenylacetic acid degradation was targeted by plasmid-borne sgRNAs, resulting in near complete inhibition of growth on phenylacetic acid as the sole carbon source. This was supported by reductions in *paaA* mRNA expression. The utility of CRISPRi to probe other functions at the single cell level was demonstrated by knocking down *phbC* and *fliF*, which dramatically reduces polyhydroxybutyrate granule accumulation and motility, respectively. As a hallmark of the mini-CTX system is the broad host-range of integration, we putatively identified 67 genera of Proteobacteria that might be amenable to modification with our CRISPRi toolkit. Our CRISPRi tool kit provides a simple and rapid way to silence gene expression to produce an observable phenotype. Linking genes to functions with CRISPRi will facilitate genome editing with the goal of enhancing biotechnological capabilities while reducing *Burkholderia*'s pathogenic arsenal.

Keywords

CRISPRi, *Burkholderia*, gene silencing, genetic tool

Author contributions

STC conceived the idea and design of the research; AMH designed and cloned the dCas9 constructs; AMH and ASMZ designed the sgRNAs, assessed knockdown phenotypes, processed data, and wrote and edited the manuscript; TJL performed RT-qPCR analysis and edited the manuscript; STC supervised the work and provided financial support.

Graphical Abstract

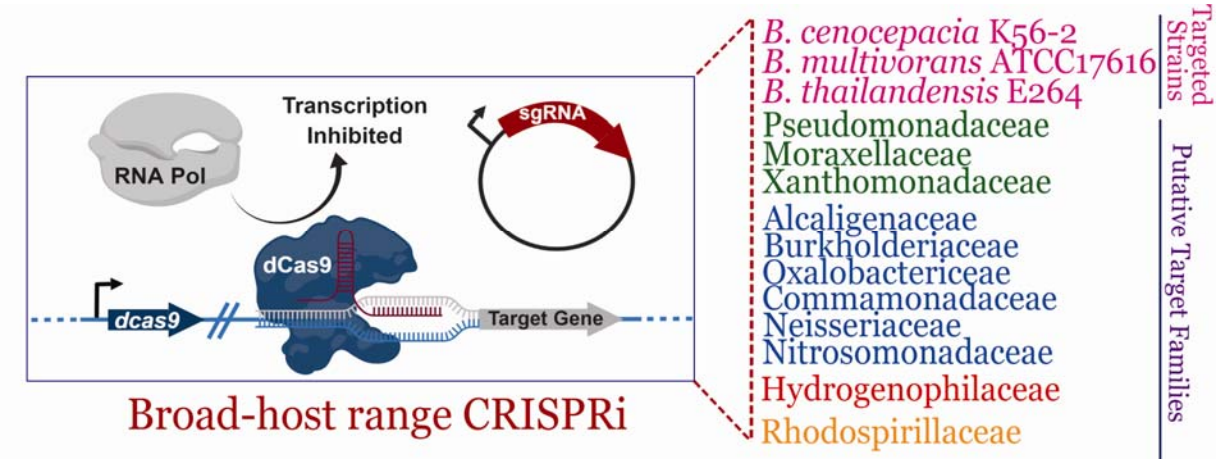

Introduction

The genus *Burkholderia* comprises a diverse group of Gram-negative bacteria characterized by a remarkable biotechnological potential, with species that can be exploited for bioremediation purposes, production of bioactive compounds, and agricultural growth promotion. Perhaps due to the phylogenetic diversity of the genus, some species of *Burkholderia* can also pose a threat to human health (Eberl and Vandamme, 2016). Within the multiple deep-branching groups of the *Burkholderia* phylogenetic tree (Depoorter et al., 2016), one branch contains the clades known as the *Burkholderia cepacia* complex (Bcc) and the *B. pseudomallei* group. The Bcc group comprises species that cause severe infections in people with the genetic disease cystic fibrosis and other patients with a compromised immune system (Mahenthiralingam et al., 2005). *B. cenocepacia* and *B. multivorans* are two relevant species of this group, which are prevalent in cystic fibrosis patients (Kenna et al., 2017). The *B. pseudomallei* group contains the risk group 3 members *B. mallei*, *B. pseudomallei*, and its close relative *B. thailandensis*, the last one being a frequent surrogate used in *B. pseudomallei* and *B. mallei* research (Howe et al., 1971). Other branches, such as the *B. xenovorans* group comprise species isolated from diverse environmental sources, like polluted soils, and plant rhizospheres (Depoorter et al., 2016). While species with and without pathogenic potential tend to cluster separately in most phylogenetic trees, the genetic characteristics that define the pathogenic potential of *Burkholderia* are poorly understood. Environmental species can cause serious infections (Nally et al., 2018), calling for caution in the use of *Burkholderia* strains for biotechnological applications. The incomplete understanding of *Burkholderia* pathogenic potential may be related to the limited tools available to link gene to function. Most genome editing methods designed for Gram-negative bacteria are inefficient in *Burkholderia* due in part

to their high resistance to the antibiotics used as genetic markers (Rhodes and Schweizer, 2016), and the high GC content of their large genomes.

Tools that facilitate controlled gene expression are necessary for interrogation of gene function. Programmable control of gene expression by promoter replacement is a valuable tool to link gene to phenotype (Judson and Mekalanos, 2000). Yet, promoter replacement implies that the natural regulatory circuitry of the target gene is interrupted. Instead, clustered regularly interspaced short palindromic repeats interference (CRISPRi) (Qi et al., 2013) is a method of silencing native gene expression, which is based on a dead Cas9 (dCas9) and a nuclease-inactive version of the RNA-guided endonuclease Cas9 (Cho et al., 2013). In CRISPRi, a single guide RNA (sgRNA) designed towards the 5' end of the target gene and the dCas9 protein form an RNA-protein complex that recognizes the target region by base-pairing, and sterically blocks transcription initiation, if targeting the promoter, or elongation if targeting downstream of the promoter, by the RNA polymerase (Qi et al., 2013). Initially developed in *Escherichia coli*, CRISPRi technology has been applied to functionally characterize genomes of a handful of bacteria (Lee et al., 2019; Liu et al., 2017; Peters et al., 2016). To achieve genome-wide control of gene expression, a wide range of dCas9 expression levels are necessary, which can be provided by expressing *dcas9* with strong inducible promoters (Peters et al., 2016) or by providing multiple copies of *dcas9* engineered in a plasmid (Lee et al., 2019). Limitations to the success of these genomic efforts are the proteotoxicity of dCas9 when expressed at high levels (Cui et al., 2018) and the necessity of customizing CRISPRi delivery tools across bacteria. Recently, the use of Tn*7* transposon mutagenesis, which specifically delivers genetic constructs close to a single *glmS* site (Choi and Schweizer, 2006; Choi et al., 2005) was applied to deliver a mobile CRISPRi system across bacteria (Peters et al., 2019). However, the Tn*7* system is less

suitable for *Burkholderia* species as their genomes contain multiple copies of *glmS*, requiring additional steps to confirm the site of chromosomal integration (Choi et al., 2006).

In this work, we employ a mini-CTX-derived mutagenesis system (Hoang et al., 2000) to achieve specific chromosomal delivery of *dcas9* in three species of *Burkholderia*, *B. cenocepacia*, *B. thailandensis* and *B. multivorans*. By placing the chromosomal copy of *dcas9* under the control of the *E. coli* rhamnose-inducible promoter (Cardona and Valvano, 2005), we demonstrate durable and tunable control of endogenous gene expression in *Burkholderia* species, which affects cellular function producing observable phenotypes. We extend the usability of our CRISPRi tool kit by exploring other bacterial genomes for putative mini-CTX insertion sites.

Results

Construction of CRISPRi system

The dCas9 from *Streptococcus pyogenes* has been shown to provide robust gene repression in diverse bacteria (Peters et al., 2016, 2019; Qi et al., 2013); we therefore selected it as our first approach. To function, the dCas9 binds a sgRNA and, by complementary base pairing, is guided to target and silences a gene of interest by sterically blocking the RNA polymerase (Qi et al., 2013). However, the genome of *S. pyogenes* has low GC-content (~40%), and from inspection of the *dcas9* gene, we expected poor codon usage in high GC-content organisms such as *Burkholderia* (67%) and subsequently low levels of expression. Indeed, we did not observe detectable levels of dCas9 by immunoblot upon expression of the native gene from *S. pyogenes* from a single copy in the *B. cenocepacia* K56-2 chromosome (Supplemental Figure 1). Upon codon optimization for *B. cenocepacia*, we first introduced the gene into a

multicopy plasmid under the control of the rhamnose-inducible promoter (Cardona and Valvano, 2005); however, we observed a severe growth defect upon induction, except at minute concentrations of rhamnose (Supplemental Figure 2A). Growth inhibition was not observed in the vector control (Supplemental Figure 2B) and it remains unclear if the inhibitory effect of dCas9 expression on growth was caused by metabolic load from expression of a large protein in multicopy, or from proteotoxicity (Rock et al., 2017).

A single chromosomal copy of *dcas9* may provide sufficient levels of expression as observed previously (Choudhary et al., 2015; Peters et al., 2016, 2019). Using the mini-CTX system, we introduced a single copy of *dcas9* under control of the rhamnose-inducible promoter into *B. cenocepacia* K56-2 (Supplemental Figure 3A and B). We observed titratable dCas9 expression at various levels of rhamnose by immunoblot (Figure 1A and Supplemental Figure 4). At rhamnose concentrations up to 1% there was no growth defect in K56-2::dCas9 (Figure 1B) or K56-2::dCas9 with non-genome targeting sgRNA (pgRNA-non-target) (Figure 1C) compared to the vector control mutant (Figure 1D).

Tunable and durable CRISPRi silencing of paaA suppresses growth on phenylacetic acid

To evaluate the utility of the CRISPRi system for gene repression in *B. cenocepacia* K56-2, we first chose to target the *paaA* gene, which encodes phenylacetate-CoA oxygenase subunit PaaA (Teufel et al., 2010). This gene, and the rest of the *paaABCDE* operon, enable growth with phenylacetic acid (PA) as a sole carbon source in *B. cenocepacia* K56-2 (Pribytkova et al., 2014), with the lack of growth being a clearly observable phenotype when the *paaA* gene is disrupted. In addition, as this is the first characterization of CRISPRi in *Burkholderia*, we also wished to assess the effect on repression efficiency when targeting the non-template (NT) and template (T) strands, as previous studies have demonstrated profound differences (Bikard et al.,

2013; Qi et al., 2013). We therefore designed five sgRNAs: three sgRNAs targeted the promoter elements and adjacent to the transcription start site (TSS) on the NT strand (sgRNA 1, 2 and 3), one sgRNA targeted near the start codon of *paaA* on the NT strand (sgRNA 4), and one sgRNA targeted near the start codon of *paaA* on the T strand (sgRNA 5) (Figure 2A).

For phenotypic characterization of the *paaA* mutants, we used M9 minimal medium with PA (M9+PA) as the sole carbon source. Upon induction of dCas9, the growth of all mutants (except the controls) was suppressed approximately 30-fold (Figure 2B) to the same level of a Δ*paaABCDE* mutant, which is unable to utilize PA as a sole carbon source (Pribytkova et al., 2014). Furthermore, in the absence of rhamnose all of the mutants grew at or near wild-type levels, suggesting that *dcas9* expression is tightly repressed in non-inducing conditions. Phenotypically, we did not observe a differential effect of placement of the sgRNA-binding site, as the growth of all mutants was suppressed equally. We also found there were no differences in control strains; mutants expressing dCas9 and either a guideless or non-targeting sgRNA displayed the same levels of growth. However, RT-qPCR demonstrated that while growth was suppressed equally in the mutants, there were sgRNA-dependent differences in gene expression levels (Figure 2C). At 0.2% rhamnose, sgRNA4, targeting near the start codon of *paaA* on the NT strand, was the most effective in suppressing *paaA* mRNA expression (~114-fold suppression), whereas sgRNA1 and sgRNA5 only had ~63-fold and ~51-fold suppression, respectively (Figure 2C). In the absence of rhamnose there was no difference in gene expression levels between the mutants and wild type confirming that the *dcas9* is tightly regulated in non-inducing conditions.

Next, we sought to determine the tunability of our CRISPRi system in *Burkholderia*. Tuning is useful to control the level of transcriptional inhibition when precision is required, such

as in the study of essential genes. To that end, we examined the growth of the dCas9 mutant of *B. cenocepacia* K56-2 with the sgRNA1 (targeting *paaA*), using PA as a sole carbon source in the presence of a 2-fold serial dilution of rhamnose. The results showed that our CRISPRi system is tunable, exhibiting growth reduction in a dose-dependent manner with variable repression across sub-saturating rhamnose concentrations (Figure 2D). We observed a nearly 30-fold repression in OD_{600nm} at concentrations well below maximum induction as identified by immunoblot, suggesting our system produces more dCas9 than is required for maximum repression as observed by this phenotype. Contrary to what had been observed in rich medium (Figure 1B and C), all dCas9 mutants (with or without the sgRNA) showed a growth defect in M9+PA above 0.2% rhamnose (Figure 2D). A similar phenomenon was also seen in M9+glycerol (data not shown). Intermediate levels of growth were observed in concentrations of rhamnose between 0.00625% and 0.05%. For consistency, we therefore used 0.2% rhamnose for dCas9 induction in all experiments.

Although once rhamnose is removed from the culture, expression of dCas9 is no longer induced, it remained possible that the dCas9 already synthesized may persist and cause long-term, or durable, silencing. To address this, the mutant strains harbouring sgRNAs targeting *paaA*, were grown overnight in rich medium with 0.2% rhamnose, effectively priming the cells with dCas9. When grown in M9+PA with and without rhamnose, we again observed strong repression of growth (~30-fold) in all conditions regardless of the presence of rhamnose in the M9+PA, and at levels similar to the Δ*paaABCDE* mutant (Figure 2E). This suggests that after the inducer is removed, dCas9 is either slowly degraded in K56-2 or is present at high enough levels in the cells for durable repression.

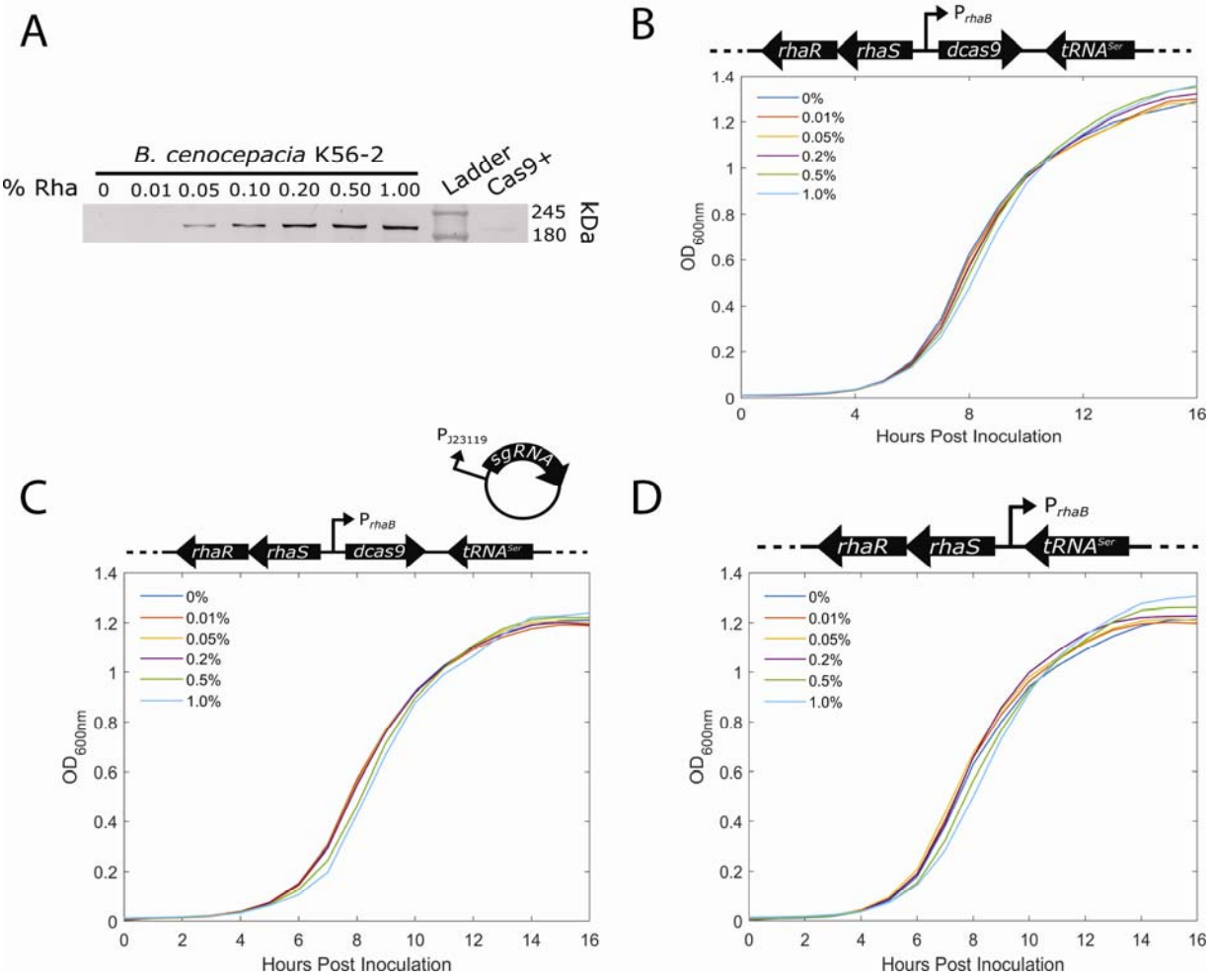

183

184 **Figure 1. Development of CRISPRi in *B. cenocepacia* K56-2**. A) dCas9 was expressed from
185 the chromosome of K56-2 under a rhamnose inducible promoter. Cells were grown to OD_{600nm} of
186 0.6 then induced with rhamnose for three hours. The soluble protein fraction was run on an 8%
187 SDS gel. dCas9 was detected by an α-dCas9 antibody followed by a second antibody linked to
188 alkaline phosphatase. B, C and D) Growth curves of *B. cenocepacia* K56-2::dCas9 (B), dCas9
189 expressed with a non-genome targeting sgRNA (dCas9/pgRNA-non target) (C) and K56-
190 2::CTX1-rha, the vector control plasmid for the integration (D) in LB media show that
191 expression of the chromosomally-encoded dCas9 induced with rhamnose up to 1% does not
192 affect growth.

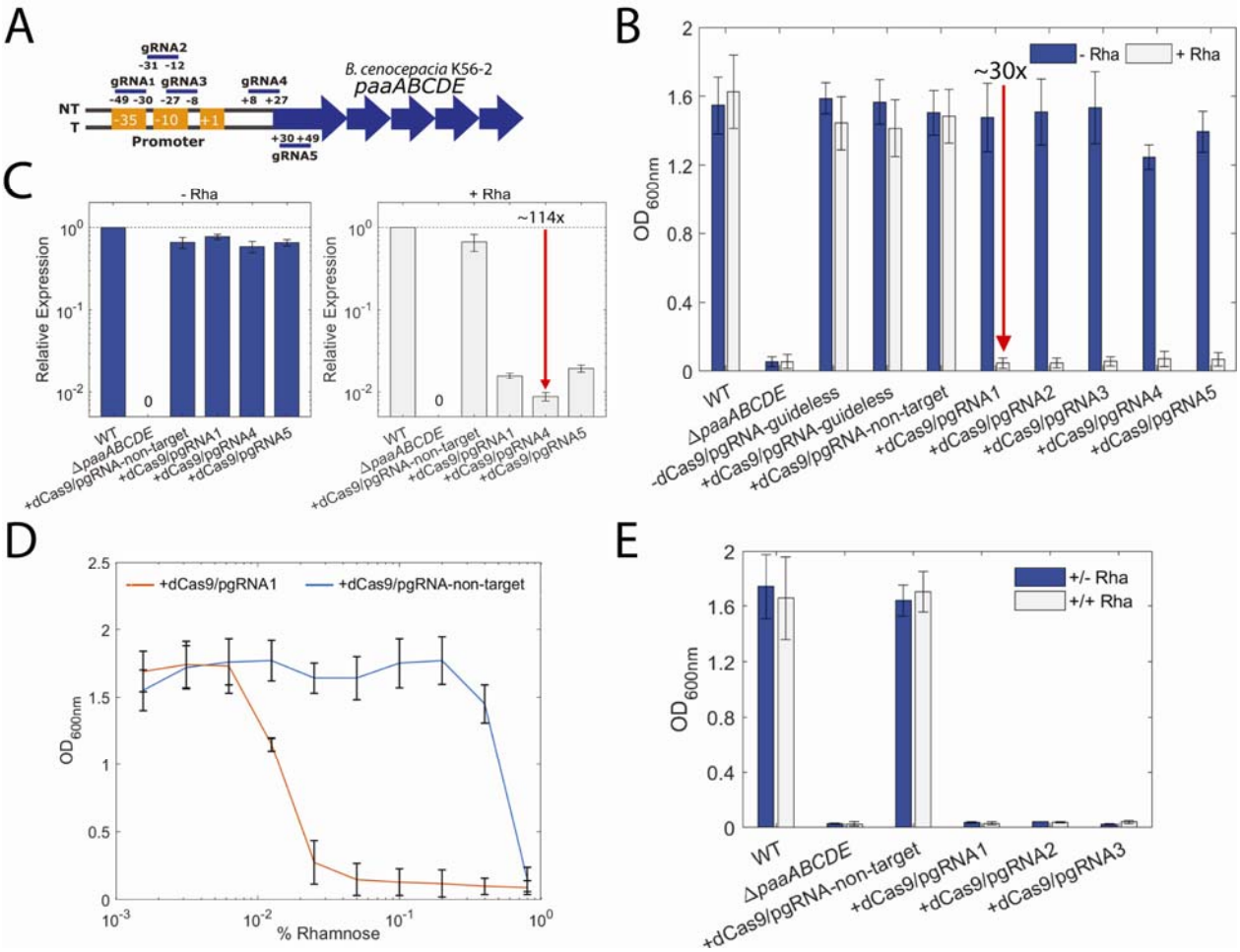

Figure 2. Targeting *paaA* with CRISPRi effectively suppresses growth in phenylacetic acid as the sole carbon source in *B. cenocepacia* K56-2. A) Positions of the sgRNAs targeting different regions upstream of and on *paaA*. sgRNAs 1, 2, and 3 were designed to target the promoter elements (-35 and -10 boxes) on the non-template (NT) strand. gRNA4 targeted the start codon on the NT strand and gRNA5 targeted the downstream region adjacent to the start codon on the T strand. B) CRISPRi blocks transcription in a strand non-specific manner. WT, a mutant of the *paaABCDE* operon (Δ*paaABCDE*), K56-2::CTX1-rha (-dCas9) and K56-2::dCas9 (+dCas9) harboring pgRNA with or without specific gRNAs were grown for 24 hours in minimal medium with PA (M9+PA) without (-Rha) or with 0.2% rhamnose (+Rha). C) RT-qPCR revealed a ~114-fold reduction in paaA mRNA, demonstrating a robust knockdown of *paaA* expression in

K56-2. D) Expression of the dCas9 can be controlled by varying the amount of inducer added to the medium, providing tunability to the CRISPRi system. However, high level induction of dCas9 with rhamnose (0.4% and beyond) was lethal for the non-genome targeting mutant (dCas9/pgRNA-non-target) expressing dCas9. E) Cells were grown overnight in LB medium with 0.2% rhamnose to induce expression of dCas9. Then cells were transferred to fresh medium and grown with (+/+ Rha) and without (+/- Rha) 0.2% rhamnose. All the values are the average of three independent biological replicates; error bars represent arithmetic mean ± SD.

Single-cell analysis reveals an 'all or none' effect in B. cenocepacia K56-2

While at the culture level the effect of CRISPRi is tunable, we further explored the effect of maximum dCas9 induction at the single-cell level. We therefore targeted *fliF*, a gene encoding a transmembrane protein that forms both the S and M rings (MS ring) of the basal body complex of the flagellum (Francis et al., 1992). Silencing *fliF* should result in non-flagellated cells as FliF is required for flagellum formation (Yang et al., 2017). We targeted *fliF* by introducing four sgRNAs designed to bind near the putative promoter and start codon on the NT strand (Supplemental Figure 5A). Our goal was to assess individual cell flagellation and compare it with swimming motility at the population level. While we observed effective inhibition of swimming motility compared to controls in a plate-based assay (approximately 5-fold reduction) (Supplemental Figure 5B and C), we were unable to observe flagella in any of the mutants harbouring gRNAs targeting *fliF* (Supplemental Figure 5D). It is possible that interfering with *fliF* expression rendered fragile flagella that could not remained attached to the cell during the staining process, while still being functional when grown in culture (Komatsu et al., 2016). In contrast to the swimming motility of the CRISPRi mutants we confirmed that insertional inactivation of *fliF* (*fliF*::pAH26) completely ablates swimming motility, as seen previously (Tomich et al., 2002).

To further elucidate the effect of CRISPRi at the single cell level, we targeted *phbC*, a gene encoding poly-β-hydroxybutyrate polymerase, an enzyme required for PHB synthesis. To repress *phbC* expression, we designed three sgRNAs to target the region up to 50 bp before the start codon on the NT strand, at the putative promoter site (Figure 3A). Polyhydroxyalkanoate (PHA) granule accumulation was assessed by fluorescence microscopy with Nile Red staining after overnight induction with rhamnose. For comparison to a null phenotype, we created a *phbC*

insertional mutant (*phbC*::pAH27) which was unable to produce PHA granules (Figure 3B and D). Compared to the wild-type and non-target controls, markedly few cells harbouring sgRNAs targeting *phbC* contained PHA granules, ranging from 17-70% depending on the sgRNA (Figure 3B). sgRNA6 rendered the strongest level of repression, with only 17.1% of cells containing PHA granules in contrast to 86.9% for the wild-type (Figure 3B). Interestingly, although few cells possessed PHA granules, the granules were of identical size to those in wild-type cells, averaging 0.65μm in diameter (Figure 3C and D). As shown by the insertional mutant, inactivation of *phbC* ablates PHA granule accumulation; therefore, the presence of granules of the same size in the dCas9 mutants as in the wild-type is indicative of an 'all-or-none' effect in *B. cenocepacia* K56-2, where most cells display the silenced phenotype, but some manage to escape the effect of CRISPRi.

Broad host range of the mini-CTX system extends applicability to other species

Having shown that the *S. pyogenes* dCas9 renders strong gene repression in *B. cenocepacia* K56-2, we next turned our attention to other important species of *Burkholderia*. We introduced the codon-optimized *dcas9* gene into the chromosome of *B. multivorans* ATCC 17616 and targeted the *paaA* and *phbC* genes by designing three sgRNAs for each centered around the putative promoter (Figures 4A and C). Targeted repression of *paaA* by each of the three sgRNAs strongly suppressed growth in M9+PA by approximately 25-fold (Figure 4B), very similar to the activity observed in *B. cenocepacia* K56-2. However, we were unable to detect robust expression of dCas9 by immunoblot in *B. multivorans* ATCC17616 (Supplemental Figure 6A). Given that the observed phenotype is indicative of effective gene silencing, it is unlikely that the actual expression of dCas9 in *B. multivorans* ATCC17616 is as low as detected

by immunoblot; however, the basis for this discrepancy is unknown. Expression of dCas9 in the presence of the non-targeting sgRNA did not affect growth in *B. multivorans* ATCC 17616 (Supplemental Figure 6B). Following this, targeting

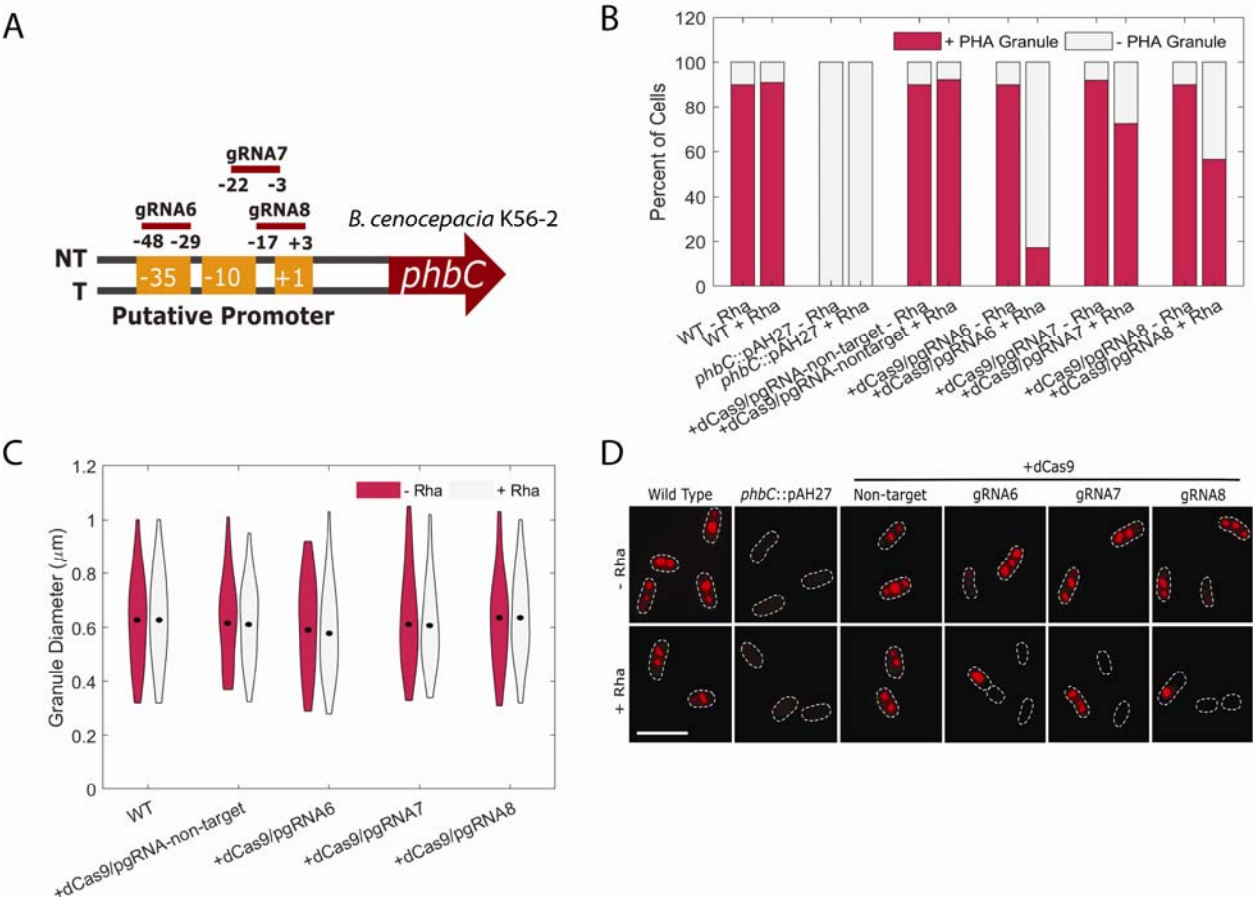

Figure 3. Targeting *phbC* with CRISPRi reduces polyhydroxyalkanoate (PHA) granule accumulation in K56-2. A) Positions of the sgRNAs targeting different regions upstream of *phbC*. sgRNAs 6, 7, and 8 were designed to target the promoter elements (-35 and -10 boxes) on the non-template (NT) strand. B) CRISPRi reduces but does not completely abrogate the number of cells with PHA granules. WT, an insertional mutant of the *phbC* gene (*phbC*::pAH27), K56-2::CTX1-rha (-dCas9) and K56-2::dCas9 (+dCas9) harboring pgRNA with or without specific gRNAs were grown overnight without (-Rha) or with 0.2% rhamnose (+Rha). Cells were washed

and stained with Nile Red, and observed by fluorescence microscopy. One to two-hundred cells were counted and the % of cells with PHA granules was calculated. C) PHA granules that remain are identical to those in the WT. Strains were grown and processed as for B and the diameter of the PHA granules was measured. Thicker areas of the violin bars represent more granules with that diameter. The mean in each condition is shown by a black dot. D) The strains were grown and processed as for B). Dashes indicate cell boundaries and the scale bar is 5 μm.

phbC rendered relatively poor inhibition of PHA granule accumulation with between 35-50% of cells containing PHA granules, depending on the sgRNA (Figure 4C and D). In contrast to what was seen in *B. cenocepacia* K56-2, we observed granules of reduced size (Figure 4E and F).

Members of the *B. pseudomallei* group are phylogenetically distinct from the Bcc (Eberl and Vandamme, 2016), but remain of interest due to the ability to cause infection (such as melioidosis and glanders) and for their remarkable capacity for secondary metabolite production (Mao et al., 2017). *B. thailandensis* is a commonly used model for the pathogenic members of the *B. pseudomallei* group, we therefore also introduced the codon-optimized *dcas9* gene into the chromosome of *B. thailandensis* strain E264. When induced with rhamnose, dCas9 was highly expressed (Supplemental Figure 6A) and did not impair growth in the presence of a non-targeting sgRNA (Supplemental Figure 6B). Similarly, as for *B. cenocepacia* K56-2 and *B. multivorans* ATCC 17616, we designed three sgRNAs targeting the putative promoters of the *paaA* and *phbC* genes (Figure 5A and C). Upon induction of dCas9 with 0.2% rhamnose, growth of the mutants harbouring the *paaA*-targeting sgRNAs was suppressed in M9+PA to varying levels ranging from 3-fold (sgRNA19) to 25-fold (sgRNA20) (Figure 5B). Lastly, for the sgRNAs targeting *phbC*, the results mirror those seen in ATCC 17616, as depending on the sgRNA there was variation in the percent of cells with PHA granules (10-40%) and the diameter of the granules (overall decrease in size) (Figure 5C- F). Though the exact contributions to PHA synthesis in E264 remain unclear, it has been previously suggested that PhbC is not the only polyhydroxyalkanoate polymerase in E264 (Funston et al., 2017).

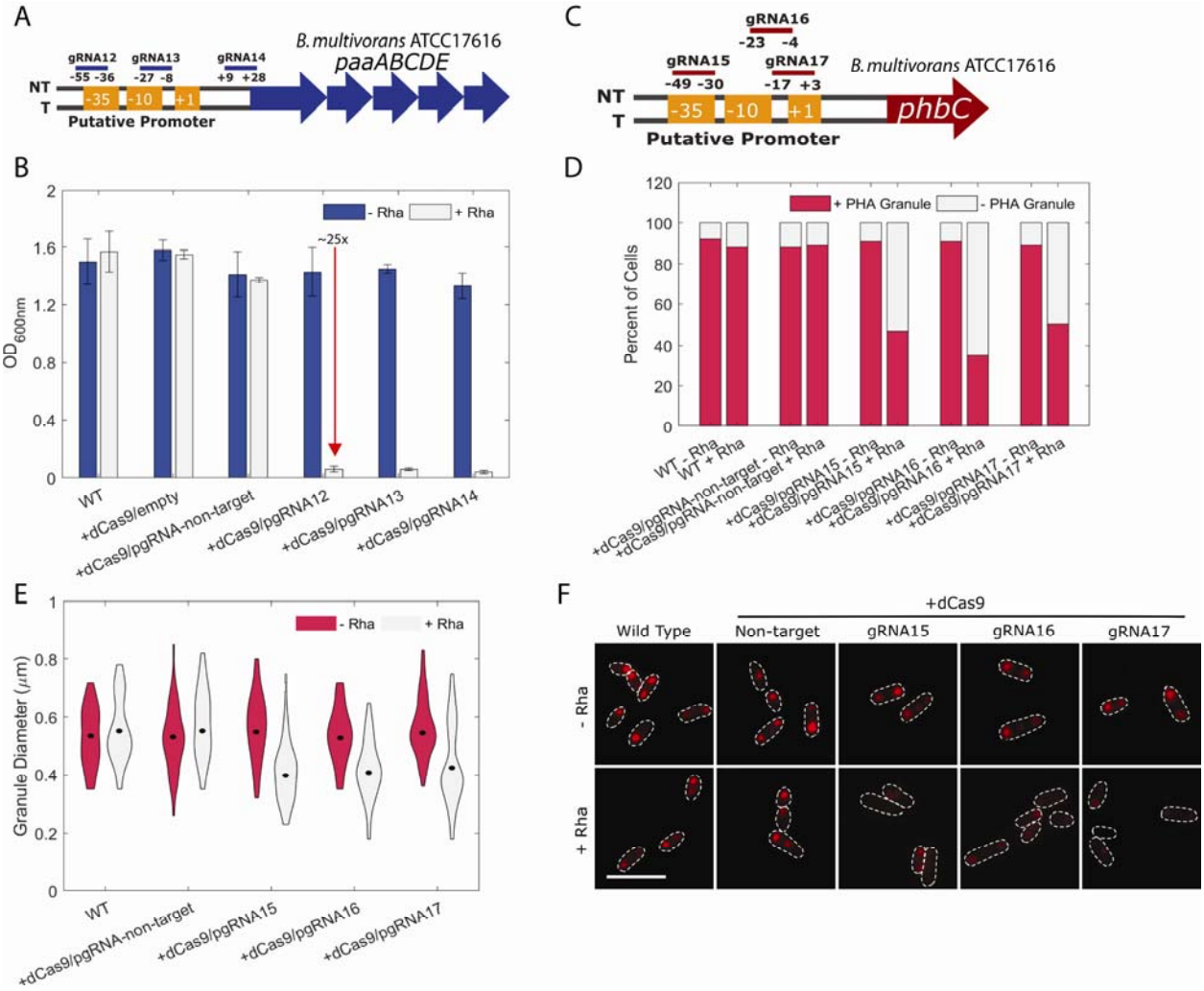

Figure 4. CRISPRi in *B. multivorans* ATCC17616 effectively represses *paaA* and *phbC*. A) Positions of the sgRNAs targeting upstream regions of *paaA*. sgRNAs12 and 13 were designed to target the -35 and -10 boxes of the promoter, while sgRNA14 targeted the 5' region of the ORF. All sgRNAs targeted the NT strand. B) Targeting *paaA* suppressed growth on PA as a sole carbon source. WT, ATCC 17616::dCas9 (+dCas9) with or without sgRNAs in A) were grown for 24 hours in M9+PA without (-Rha) or with 0.2% rhamnose (+Rha). C) Positions of the sgRNAs targeting upstream regions of *phbC*. All sgRNAs were designed to target the -35 or -10 elements of the promoter on the NT strand. D) Targeting *phbC* reduces the overall number of cells with PHA granules. Strains were grown overnight without (-Rha) or with 0.2% rhamnose

(+Rha). Cells were washed and stained with Nile Red, and observed by fluorescence microscopy. One to two-hundred cells were counted and the % of cells with PHA granules was calculated. E) PHA granules that remain are smaller than those in the WT. Strains were grown and processed as for D); however, the diameter of the PHA granules was measured, with thicker areas representing more granules with that diameter. The mean in each condition is shown by a black dot. F) The strains were grown and processed as for D). Dashes indicate cell boundaries and the scale bar is 5 μm.

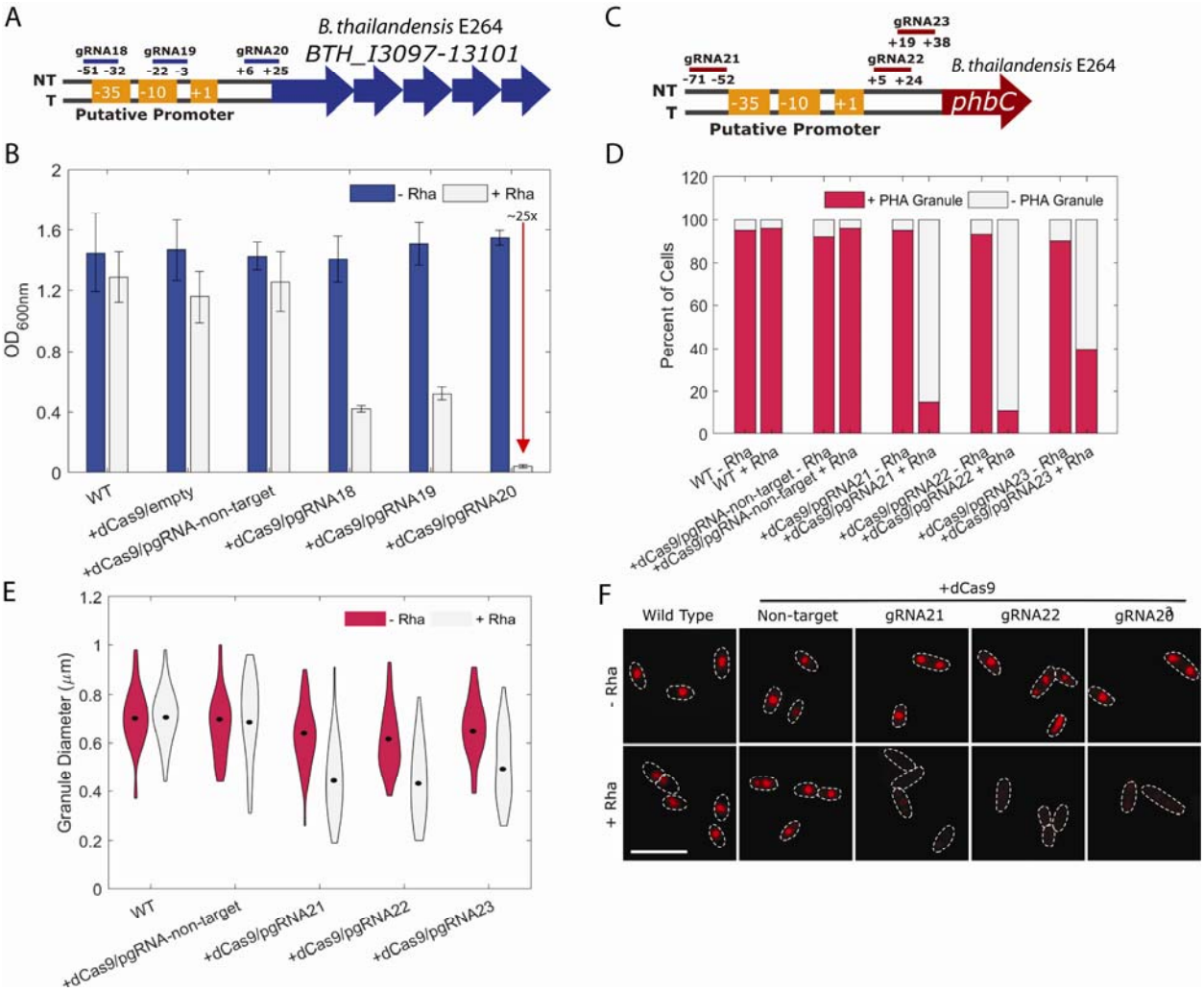

Figure 5. CRISPRi in *B. thailandensis* E264 effectively represses *paaA* (BTH_I3097) and *phbC*. Positions of the sgRNAs targeting upstream regions of *paaA* (BTH_I3097). sgRNAs 18 and 19 were designed to target the -35 and -10 boxes of the promoter, while sgRNA 20 targeted the 5' region of the ORF. All sgRNAs targeted the NT strand. B) Targeting *paaA* suppressed growth on PA as a sole carbon source. WT, E264::dCas9 (+dCas9) with or without sgRNAs in A) were grown for 48 hours in M9+PA without (-Rha) or with 0.2% rhamnose (+Rha). C) Positions of the sgRNAs targeting regions of *phbC*. sgRNA 21 targeted just upstream of the -35

box, sgRNA22 and 23 targeted just downstream of the -10 box, all on the NT strand. D) Targeting *phbC* reduces the overall number of cells with PHA granules. Strains were grown overnight without (-Rha) or with 0.2% rhamnose (+Rha). Cells were washed and stained with Nile red, and observed by fluorescence microscopy. One to two-hundred cells were counted and the % of cells with PHA granules was calculated. E) PHA granules that remain are smaller than those in the WT. Strains were grown and processed as for D); however, the diameter of the PHA granules was measured, with thicker areas representing more granules with that diameter. The mean in each condition is shown by a black dot. F) The strains were grown and processed as for D). Dashes indicate cell boundaries and the scale bar is 5 μm.

The integration vector we implemented to deliver *dcas9* to the chromosome of various species of *Burkholderia* relies on the expression of the φCTX integrase and recombination using the plasmid-borne *attP* site with the chromosomal *attB* site (Hoang et al., 2000). φCTX is a *Pseudomonas*-infecting phage, and the mini-CTX integration system was originally designed for use in *P. aeruginosa* (Hoang et al., 2000). The mini-CTX integration system has been used successfully in other species; however, this has been mostly limited to members of *Burkholderia* (Chapalain et al., 2017; Le Guillouzer et al., 2017). The utility in *Burkholderia* has been comparable to *P. aeruginosa*, in part owing to efficient integration. In the species used in this study, we observed the integration efficiencies to be $6x10^{-7}$ in K56-2, $6x10^{-8}$ in E264, and $5x10^{-9}$ in ATCC 17616 (Supplemental Figure 7A), compared to 10^{-7} to 10^{-8} observed previously in *P. aeruginosa* (Hoang et al., 2000). To further broaden the scope of the applicability of our CRISPRi system, we used NCBI BLAST to search all published genomes for putative *attB* sites. While the full-length *attB* site is 30 nt, integration is known to occur if only the 5' 19 nt are completely complementary, such as for many species of *Burkholderia*. This shorter *attB* site was therefore used as a BLAST query, resulting in 1760 hits with 100% alignment (Supplementary Table 5). Enterobacteria were excluded from the search as the pMB1 *oriR* in the mini-CTX system is functional is these species; therefore, integrants cannot be easily isolated. Furthermore, the search parameters were modified to only include species of Proteobacteria, as there were few hits of non-Proteobacterial species with 100% alignment (data not shown). Overall, there were 168 unique species from 67 genera. As expected, the most abundant hit corresponded to species and strains of *Pseudomonas* (480 hits), then followed by *Acinetobacter* (443 hits), *Burkholderia* (276 hits), *Neisseria* (170 hits), and *Ralstonia* (146 hits), with members of the other 62 genera comprising the remaining 245 hits. A summary of the major hits and species of interest

(pathogenic, environmental, biotechnological, etc.) can be found along with the genomic context in Table 1. We note that the hit table comprises species with both high and low GC-content genomes, and while the GC-rich codon-optimized *dcas9* (in pAH-CTX1-rhadCas9) may be better suited for species with high GC-content genomes, such as those in the families *Pseudomonadaceae* and *Alcaligenaceae*, the native *dcas9* (in pAH-CTX1-rhadCas9-native) may have better functionality in species with low GC-content genomes, such as those in the families *Moraxellaceae* and *Neisseriaceae*.

A further consideration for use of our CRISPRi system is that the pFLPe recombinase-expressing plasmids might not be functional in all species. In which case, the *int* and *tet* genes along with the *oriT* and pBM1 *oriR* would not be excised and the mutant would remain resistant to tetracycline. To explore if experiments could be performed in the absence of tetracycline selection, we assessed the stability of the mini-CTX integration in K56-2, ATCC 17616, and E264 in serial passages over four days without tetracycline. For all species over the entire experiment we determined CFU counts on agar with and without tetracycline selection and found equal recovery of tetracycline-resistant colonies as total colonies (Supplemental Figure 7B-D), suggesting the integration is stable.

Table 1. Putative host range of the mini-CTX system and genomic context of selected hit sites

Class	Order	Family	Genus and Species	Strain	%GC	tRNA^{Ser} ( ) Genomic Context
Gammaproteobacteria	Pseudomonadales	Pseudomonadaceae	*Pseudomonas aeruginosa*	PAO1	66.6	
			Pseudomonas fluorescens	NCTC 10783	65.9	
			Pseudomonas mendocina	NK-01	64.7	
		Moraxellaceae	*Acinetobacter baumannii*	ATCC 17978	39	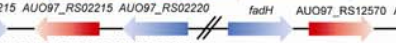
			Acinetobacter nosocomialis	NCTC 8102	38.7	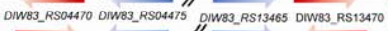
	Xanthomonadales	Xanthomonadaceae	*Xylella fastidiosa*	M12	51.9	
Betaproteobacteria	Burkholderiales	Alcaligenaceae	*Achromobacter xylosoxidans*	NCTC 10808	67.4	
			Bordatella bronchiseptica	D448	68.1	
			Alcaligenes faecalis	DSM 30030	56.6	
		Burkholderiaceae	*Ralstonia pickettii*	DTP0602	65.9	
			Burkholderia cenocepacia	K56-2	67	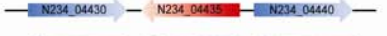
			Burkholderia multivorans	ATCC 17616	66.7	
			Burkholderia thailandensis	E264	67.7	
			Burkholderia mallei	NCTC 10229	68.5	
			Burkholderia pseudomallei	NCTC 13178	67.9	
			Burkholderia oklahomensis	EO147	66.9	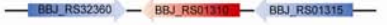
			Cupriavidus necator	NH9	65.5	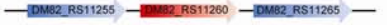
			Pandoraea apista	AU2161	62.6	
			Lautropia mirabilis	NCTC 12852	65.5	
		Oxalobactericeae	*Collimonas fungivorans*	Ter6	59	
		Commamonadaceae	*Rhodoferax antarcticus*	DSM 24876	58.9	
			Polaromonas naphthalenivorans	CJ2	61.7	
	Neisseriales	Neisseriaceae	*Neisseria meningitidis*	NCTC 10026	51.4	
			Neisseria gonorrheae	NCTC 13484	52.5	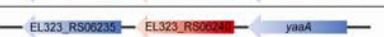
			Neisseria sicca	FDAARGOS_260	50.9	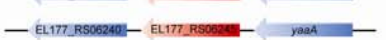
			Chromobacterium violaceum	CV1197	65.6	
	Nitrosomonadales	Nitrosomonadaceae	*Nitrosomonas communis*	Nm2	44.7	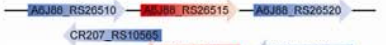
Hydrogenophilalia	Hydrogenophilales	Hydrogenophilaceae	*Hydrogenophilus thermoluteolus*	TH-1	61.7	
Alphaproteobacteria	Rhodospirillales	Rhodospirillaceae	*Haematospirillum jordaniae*	H5569	55.6	

Discussion

Genetic tools are necessary to dissect the molecular mechanisms governing cellular processes. Here, we report the development of a CRISPRi system for efficient repression of gene expression in *Burkholderia*. By mobilizing the *dcas9* gene that was codon-optimized for the GC-rich *Burkholderia* on a broad host range mini-CTX1 integration vector, we demonstrate robust, tunable, and durable repression of endogenous genes. While others have shown effective repression using the native *dcas9* gene in *E. coli* (Qi et al., 2013), *B. subtilis* (Peters et al., 2016), *Staphylococcus aureus*, and *Acinetobacter baumannii* (Peters et al., 2019), codon-optimization was a necessary step for K56-2, as expression of the native *dcas9* gene was not detectable in K56-2. Indeed, for expression in species with high GC-content, codon optimization appears to be necessary. In *P. aeruginosa* (66.3% GC) both the *S. pyogenes* dCas9 (Peters et al., 2019) and the *S. pasteurianus* dCas9 (Tan et al., 2018) were not expressed unless first codon-optimized, albeit for *Mycobacterium* (~67% GC) or *Homo sapiens* (optimized at 50.2% GC). Additionally, the *S. thermophilus* dCas9 was codon-optimized for *Mycobacterium* for efficient expression in *M. tuberculosis* and *M. smegmatis* (Rock et al., 2017).

Upon codon-optimizing the *dcas9* gene, we observed a severe growth defect when expressed from a multicopy pBBR1 origin plasmid. At this time, we are unsure if this was caused by a metabolic burden of expressing a large protein from a multicopy plasmid or from direct proteotoxicity. Previous studies have demonstrated that expression of the canonical *S. pyogenes* dCas9 causes toxicity in *M. smegmatis*, *M. tuberculosis* (Rock et al., 2017), and *E. coli* (Cho et al., 2018), which provides rationale for developing a system with low-enough levels of dCas9 expression to maintain cell viability without sacrificing repression activity. While this effort has spurred the exploration of alternative dCas9 orthologues (Rock et al., 2017), we found

that introducing *dcas9* in single copy in the chromosome provided a balance of repression activity without affecting growth. Furthermore, while other systems display up to 3-fold repression in the absence of inducer (Peters et al., 2016; Tan et al., 2018), our application of the tightly regulated rhamnose-inducible promoter from *E. coli* does not display such a phenomenon in any of the three species tested. However, with the benefit of apparently negligible uninduced expression, the rhamnose-inducible promoter is incapable of attaining the high levels of maximal expression seen in other systems, such as the xylose-inducible promoter used in the *B. subtilis* CRISPRi library (Peters et al., 2016) (Supplementary Figure 4A). While we did observe increased dCas9 expression at rhamnose concentrations of 0.5% and 1.0% with no inhibitory effect on growth in LB (Figure 1C and D), the increased level of dCas9 expression was accompanied by a substantial growth defect in M9 minimal media with PA (Figure 2D) or glycerol (data not shown) as the sole carbon source. As the growth rate is decreased in minimal media, it is possible that growth inhibitory, off-target effects that are alleviated in fast growing cells by dilution of dCas9 bound DNA sites with newly replicated ones, are more evident in slowly growing cells. While the RNA polymerase is largely incapable of displacing the dCas9:sgRNA complex, the DNA replication machinery is not blocked by dCas9. In fact, it has been observed that the dissociation of the dCas9:sgRNA complex correlates well with the generation time in *E. coli* (Jones et al., 2017). This is an important consideration for understanding the durability of growth suppression we observed when using PA as a sole carbon source. Cells primed by pre-incubation with rhamnose are unable to grow in M9+PA, creating a condition where *paaA* is an essential gene and its absence would arrest cell division and replication. Hence, the DNA replication machinery would not displace the dCas9:sgRNA from the *paaA* gene, resulting in long-term growth suppression. By extension, we predict that strong

423 knockdown of any (conditionally) essential gene that causes a halt in DNA replication would be
424 durable in this manner. This is a useful aspect of CRISPRi that we are investigating further.

425 Although it has been reported that the CRISPRi system is less effective in silencing gene
426 expression when the template strand (T) is targeted compared to the non-template (NT) strand,
427 our results demonstrated nearly 30-fold repression of the growth irrespective of the *paaA* target
428 strand (Figure 2B). This suggests that the efficiency of the CRISPRi system might not be strand
429 specific at all loci, supporting the findings from Howe et al. (Howe et al., 2017). However, this
430 effect might have been masked by the strong repression we observed, as it is difficult to compare
431 across null phenotypes. This is supported by the RT-qPCR that demonstrated differential
432 repression of gene expression based on the targeted location. Interestingly, our data suggests that,
433 for *paaA*, targeting near the start codon of the NT strand (gRNA4) was more effective than
434 targeting near the start codon of the T strand (gRNA5). Additionally, sgRNAs targeting different
435 regions of the 5' region of *paaA* produced a strong 25 to 30-fold repression in the three species
436 studied here. Therefore, the observed knockdown efficiency appears to be largely unaffected by
437 sgRNA placement on targeting regions overlapping or adjacent to the −35 and −10 promoter
438 elements, at least for phenotypes where complete suppression of gene expression is not required.
439 The cause of this is likely due to the large dCas9:sgRNA complex that when bound to the
440 promoter sterically interferes with RNA polymerase binding. Indeed, the ~160 kDa dCas9
441 enzyme has an average DNA footprint of 78.1 bp, much larger than most promoter regions
442 (Josephs et al., 2015).

443 Single cell level analysis of our system demonstrated a unimodal 'all or none' effect in
444 K56-2 with ~17% cells escaping the silenced phenotype when targeting *phbC* compared to an
445 insertion mutant, which did not possess any granules. The PHB granules in these cells were of

identical diameter to wild type, averaging 0.65µm in diameter. The 'all or none' effect might be attributed to an uneven distribution of the membrane transporter involved in transporting rhamnose into the cell, essentially escaping the rhamnose mediated *dCas9* induction to silence the target gene (Siegele and Hu, 1997). Interestingly, targeting *phbC* in *B. multivorans* ATCC17616 and *B. thailandensis* E264 resulted in a mixed phenotype with a reduced number of cells with granules as well as an overall decrease in granule size. Even though some of the cells seemed to have escaped the repression (up to 35% in ATCC17616 and 6% in E264), more than 90% of the cells contained granules of reduced size. This suggests that there is an unelucidated secondary PHA synthesis pathway in *B. thailandensis* E264 and *B. multivorans* ATCC17616. Funston et al. (Funston et al., 2017) have observed similar results in *B. thailandensis* E264 where transposon mutants in *phb* genes (*phbA*, *phbB* and *phbC*) retained the ability to synthesize PHA, albeit at lower levels.

One of the hallmarks of CRISPRi is the broad-range amenability in diverse bacteria, enabling synthetic biology and mechanistic investigations into many dozens of species in innovative ways. We wished to apply our CRISPRi system in this manner and therefore mobilized both the native *dcas9* gene, suitable for low/medium GC-content organisms, and the *dcas9* gene, codon-optimized for GC-rich *Burkholderia*, on the mini-CTX1 integration vector. Our analysis of putative hosts (with *attB* sites near the 3' end of the serine tRNA) identified 168 unique species in 67 genera, mostly from the β- and γ-Proteobacteria. Previous works have mobilized *dcas9* on broad host-range integrative plasmids (Peters et al., 2019; Tan et al., 2018); however, both systems use the mini-Tn*7* system, which has multiple insertion locations in certain genomes, such as many species of *Burkholderia*. Together, our work contributes to the available genetic toolkit for rapid functional analysis of bacteria.

Methods

Strains, selective antibiotics, and growth conditions

All strains and plasmids are found in Supplemental Table 1. All strains were grown in LB-Lennox medium (Difco). *B. cenocepacia* K56-2 and strains of *E. coli* were grown at 37°C, while *B. thailandensis* E264 and *B. multivorans* ATCC 17616 were grown at 30°C. The following selective antibiotics were used: chloramphenicol (Sigma; 100 μg/mL for *B. cenocepacia*, 20 μg/mL for *E. coli*), trimethoprim (Sigma; 100 μg/mL for strains of *Burkholderia*, 50 μg/mL for *E. coli*), tetracycline (Sigma; 50 μg/mL for all strains of *Burkholderia*, 20 μg/mL for *E. coli*), kanamycin (Fisher Scientific; 250 μg/mL for *B. thailandensis*, 150 μg/mL for *B. multivorans*, 40 μg/mL for *E. coli*), ampicillin (Sigma; 100 μg/mL for *E. coli*), gentamicin (Sigma; 50 μg/mL for all strains of *Burkholderia*).

Construction of pSC-rhadCas9, pAH-CTX1-rhadCas9, pAH-CTX1-rhadCas9-native, and dCas9 insertional mutants

The endogenous *cas9* gene from *S. pyogenes* has low GC content (averaging 34.1%) and subsequently poor codon usage for GC-rich organisms (http://www.kazusa.or.jp/codon/). The nuclease-inactive variant (*dcas9*) was therefore codon optimized for *B. cenocepacia* by purchasing the optimized gene in two fragments from IDT (2462 bp and 1849 bp, Supplemental Table 2), each with 38 bp overlapping regions. Strong, rho-independent terminators were added following the gene. The full-length gene (with terminal *Nde*I and *Hind*III cut sites) was synthesized by overlap-extension PCR using Q5 polymerase with high GC buffer (NEB) and

primers 979 and 987 (Supplemental Table 2). The first ten rounds of PCR were performed without primers to synthesize the full-length product using the overlap regions; primers were added for the following 25 cycles. The cycle parameters are as follows: 98°C for 30 sec, (98°C for 10 sec, 67.5°C for 20 sec, 72°C for 2.5 min)x10 cycles, 72°C for 5 min, 98°C for 30 sec, (98°C for 10 sec, 62.5°C for 20 sec,72 °C for 2.5 min)x25 cycles, 72°C for 10 min. The 4267 bp product was gel-purified (Qiagen) and introduced into pSCrhaB2 by restriction cloning using *Nde*I and *Hind*III (NEB). The resulting plasmid, pSC-rhadCas9, was transformed into *E. coli* DH5α, and trimethoprim-resistant colonies were screened by colony PCR with primers 954 and 955. Triparental mating with *E.* coli MM290/pRK2013 as a helper was performed as previously described (Hogan et al., 2018).

To introduce the optimized *dcas9* into the mini-CTX1 insertion plasmid (Hoang et al., 2000) serial restriction cloning was used (Supplemental Figure 3A). Briefly, the rhamnose-inducible promoter from pSC201 (Ortega et al., 2007) was first PCR amplified with Q5 polymerase and primers 976 and 1071, containing *Hind*III and *Spe*I restriction sites, respectively. This fragment was introduced into mini-CTX1, to create pAH-CTX1-rha, and tetracycline-resistant *E. coli* DH5α were screened by colony PCR using primers 957 and 1074. The fragment containing the dCas9 gene was PCR amplified as above, but instead using primers 1072 and 1073, introducing *Spe*I and *Not*I restriction sites, respectively. This fragment was introduced into pAH-CTX1-rha, to create pAH-CTX1-rhadCas9, and tetracycline-resistant *E. coli* DH5α colonies were screened by colony PCR using primers 954 and 955.

The native (non codon-optimized) *dcas9* was also introduced into pAH-CTX1-rha. The native *dcas9* and transcriptional terminators were PCR amplified from pdCas9-bacteria (Addgene plasmid # 44249) with Q5 polymerase (NEB) using primers 1216 and 1217. The PCR

product was cloned into pAH-CTX1-rha (creating pAH-CTX1-rhadcas9-native) using *Not*I and *Spe*I restriction sites then transformed into *E. coli* DH5α. Tetracycline-resistant colonies were screened by PCR using primers 954 and 1218.

pAH-CTX1-rha, pAH-CTX1-rhadCas9, and pAH-CTX1-rhadCas9-native were introduced into *Burkholderia* species by triparental mating using *E. coli* MM290/pRK2013 as a helper as above. Tetracycline-resistant colonies were screened by colony PCR using primer 954 (for pAH-CTX1-rha) or 1075 (for pAH-CTX1-rhadCas9) or 1219 (for pAH-CTX1-rhadcas9-native) and 1008 (for *B. cenocepacia*), 1167 (for *B. multivorans*), or 1168 (for *B. thailandensis*).

To remove the tetracycline resistance and integrase genes from the insertional mutants constructed with pAH-CTX1-rhadCas9 and pAH-CTX1-rha (Supplemental Figure 3), the Flannagan method (Flannagan et al., 2008) was used for *B. cenocepacia* K56-2, while and the pFLPe system (Choi et al., 2008) was used for *B. multivorans* ATCC 17616 and *B. thailandensis* E264. To remove the regions flanking the *FRT* sites in *B. cenocepacia* K56-2, a fragment with 475 bp overlapping the upstream and downstream regions of the *FRT* sites was designed and synthesized (IDT) with *Kpn*I and *Eco*RI restriction sites, respectively. The fragment was ligated into pGPI-*Sce*I (Flannagan et al., 2008) via the *Kpn*I and *Eco*RI restriction sites, creating pAH18, and transformed into *E. coli* SY327. Trimethoprim-resistant colonies were screened for the insertion of the fragment with primer 153 and 154. pAH18 was introduced into the mutant backgrounds via triparental mating, as described above. Trimethoprim-resistant K56-2 were screened by PCR for both possible integration orientations using primers 154 and 1126, or 153 and 1133. To initiate the second recombination, an *Sce*I-expressing plasmid is required; however, the conventional plasmid, pDAI-*Sce*I, confers tetracycline resistance and could not be selected for in the mutant background. Therefore, the tetracycline resistance cassette was

537 removed by digestion with *Age*I and *Xho*I. The chloramphenicol resistance gene *cat* was PCR
538 amplified from pKD3 (Datsenko and Wanner, 2000) using primers 1084 and 1150, then ligated
539 into the *Age*I and *Xho*I-digested pDAI-*Sce*I backbone and transformed into *E. coli* DH5α,
540 creating pAH25-*Sce*I. Chloramphenicol-resistant colonies were screened with primers 1091 and
541 1150. pAH25-*Sce*I was introduced into the mutant backgrounds by triparental mating as
542 described above. Chloramphenicol-resistant colonies were screened for sensitivity to
543 trimethoprim (indicating excision of pAH18) and tetracycline (indicating excision of the genes
544 between the *FRT* sites), and then screened by PCR with primers 1126 and 1133, which bridge the
545 excision.

546 The pFLPe system was used to remove the tetracycline resistance and integrase genes in
547 the dCas9 mutants in *B. multivorans* ATCC 17616 and *B. thailandensis* E264. Triparental mating
548 to introduce pFLPe4 into the strains was performed as for K56-2 above, except 0.2% rhamnose
549 was added to the mating and antibiotic selection plates. Tetracycline-sensitive colonies were
550 screened by PCR using primers 957 and 1194 (for *B. multivorans*) or 1195 (for *B. thailandensis*).
551 pFLPe4 has a temperature-sensitive origin of replication; therefore, mutants were grown
552 overnight in LB without antibiotics at 37^{o}C. Single colonies were then tested for kanamycin
553 sensitivity and then by colony PCR for pFLPe4 using primers 1128 and 1129.

554 *Design and construction of the sgRNA-expressing plasmids*

555 PAM sequences closest to the 5' end of the transcription start site (TSS) were first
556 identified on both the non-template and template strands. We extracted 20-23 nucleotides
557 adjacent to the PAM sequence to design the base-pairing region of the sgRNAs in the following
558 format: 5'-CCN-$N_{(20-23)}$-3' for targeting the non-template strand and 5'$N_{(20-23)}$-NGG-3' for the
559 template strand. To score the specificity and identify off-target binding sites, the 5' end of the

20-23nt variable base-pairing sequences were trimmed one base at a time and the remaining base-pairing region was searched against the appropriate organism's reference genome. This was repeated until only 10 nt was used as a search query. Potential sgRNAs were discarded if off-target sites were discovered in this manner.

The expression vector pSCrhaB2 (Cardona and Valvano, 2005) was chosen as the method of sgRNA expression due to the broad host range of the pBBR1 origin of replication. The sgRNA cassette from pgRNA-bacteria (Qi et al., 2013) (Addgene plasmid # 44251) was introduced into pSCrhaB2 by restriction cloning with *Eco*RI and *Hind*III (NEB) to create pSCrhaB2-sgRNA. To remove *rhaS* and *rhaR*, inverse PCR was performed using Q5 polymerase (NEB) and primers 847 and 1025. The resulting fragment was ligated by blunt-end ligation using 1μL of PCR product incubated with 0.5 μL *Dpn*I, 0.5 μL T4 polynucleotide kinase, and 0.5 μL T4 ligase (NEB) with quick ligation buffer (NEB) at 37^{o}C for 30 minutes. The resulting plasmid, pSCB2-sgRNA, was screened using primers 781 and 848, which span the ligated junction. Individual sgRNAs were introduced into pSCB2-sgRNA using inverse PCR as previously described (Qi et al., 2013) (Supplemental Table 3).

Construction of insertional mutants K56-2 fliF::pAH26 and K56-2 phbC::pAH27

Inactivation of *fliF* was performed with the mutagenesis system of Flannagan et al. (Flannagan et al., 2007). Briefly, a 322 bp internal fragment of *fliF* was PCR amplified from the K56-2 genome using primers 1156 and 1157 and Q5 polymerase (NEB). The fragment and pGPΩ-Tp were double digested with *Kpn*I and *Eco*RI (NEB) and ligated with T4 ligase (NEB). The resulting plasmid, pAH26, was electroporated into *E. coli* SY327, and trimethoprim-resistant colonies were screened by colony PCR for the *fliF* fragment. Triparental matings were

582 performed as above. Trimethoprim-resistant exconjugants, were screened by motility assay
583 (below).

584 Inactivation of *phbC* (WQ49_RS30385) was performed as for *fliF*. Briefly, a 328 bp
585 internal fragment of *phbC* was PCR amplified from the K56-2 genome using primers 1196 and
586 1197 and Q5 polymerase (NEB). The plasmid, pAH27, created from ligating the fragment into
587 pGPΩ-Tp using *Kpn*I and *Eco*RI (NEB) restriction sites, was electroporated into *E. coli* SY327
588 and trimethoprim-resistant colonies were screened by colony PCR for the *phbC* fragment.
589 Triparental matings were performed as above, and trimethoprim-resistant exconjugants were
590 screened by staining for polyhydroxyalkanoate granule accumulation (below).

591 *Assays for integration efficiency and stability of the mini-CTX1-based system*

592 To assess integration efficiency, triparental matings were started as above. However, after
593 the mating on LB agar, the pellicles were serially diluted and plated for CFU/mL on LB agar
594 with 50 μg/mL gentamicin and LB agar with 50 μg/mL tetracycline and 50 μg/mL gentamicin.

595 To assess stability of the integration, cultures of the dCas9 mutants (containing the
596 tetracycline resistance cassette) were serial passaged over 4 days without antibiotics. Each day, a
597 fresh culture was started with a 1:2500 dilution of the previous day's stationary phase culture. In
598 addition, the cultures were serially diluted and plated for CFU/mL on LB agar without antibiotics
599 and LB agar with 50 μg/mL tetracycline.

600 *Growth assay with phenylacetic acid as the sole carbon source*

601 Overnight cultures, started from isolated colonies, of the appropriate strains were washed
602 at 4000x g for 4 minutes and resuspended in PBS (2.7 mM KCl, 136.9 mM NaCl, 1.5 mM
603 KH_2PO_4, 8.9 mM Na_2HPO_4, pH 7.4) to remove growth medium. The OD_{600nm} of the cultures was

normalized to 0.01 in M9 medium supplemented with 5 mM phenylacetic acid, 100 μg/mL trimethoprim, and 0.2% rhamnose as required. The culture was added to wells of a 96-well plate and incubated with continuous shaking at 37°C (*B. cenocepacia* K56-2) or 30°C for *B. multivorans* ATCC 17616 and *B. thailandensis* E264). The OD_{600nm} of the cultures was measured after 24 hours for *B. cenocepacia* K56-2 and *B. multivorans* ATCC 17616, or 48 hours for *B. thailandensis* E264.

Fluorescent microscopy and polyhydroxyalkanoate granule detection

Overnight cultures of the appropriate strains with or without rhamnose were first washed to remove growth medium and resuspended in PBS. Cells were fixed in 3.7% formaldehyde + 1% methanol at room temperature for 10 minutes (*B. cenocepacia* K56-2) or 20 minutes (*B. multivorans* ATCC 17616 and *B. thailandensis* E264) then quenched by the addition of an equal volume of 0.5 M glycine. The cells were washed and resuspended in PBS with 0.5 μg/mL Nile Red (Carbosynth) and stained at room temperature in the dark for 20 minutes, after which the cells were washed to remove excess stain and resuspended in PBS. The cells were mounted on 1.5% agarose pads and imaged by fluorescence microscopy at 1000x total magnification on an upright AxioImager Z1 (Zeiss). Nile Red was excited at 546/12 nm and detected at 607/33 nm.

Plate-based motility assay

Assays were performed as previously described (Kumar and Cardona, 2016), with some modifications. Briefly, strains were grown on LB agar with the appropriate antibiotics and single colonies were stab-inoculated into motility medium consisting of nutrient broth (Difco) with

0.3% agar. Medium was supplemented with rhamnose (Sigma) as appropriate. Plates were incubated right-side up for 22 hours at 37°C.

Flagellum staining

Staining was performed as previously described (Kumar and Cardona, 2016). Briefly, an overnight culture was rested statically at room temperature for 20 minutes. Gently, a 1 in 10 dilution was prepared in water and rested statically for a further 20 minutes. A small drop of the diluted culture was placed on a clean glass slide and rested for 20 minutes. A coverglass was gently applied and one side was flooded with Ryu flagellum stain (Remel), then allowed to dry for 2 hours at room temperature. Slides were observed by light microscopy at 1000x total magnification on an upright AxioImager Z1 (Zeiss).

SDS-PAGE and Immunoblotting

Cells from an overnight culture were subcultured into fresh medium and grown at 37°C (30°C for *B. thailandensis*) to an OD_{600nm} of 0.4, then exposed to various concentrations of rhamnose for 3 hours. Soluble protein was isolated first by sonicating the cells in TNG Buffer (100 mM Tris-HCl, 150 mM NaCl, 10% glycerol, pH 7.4) then by centrifugation at 15 000g for 20 minutes. Following boiling denaturation in SDS loading buffer (50 mM Tris-HCl, 2% SDS, 0.2% bromophenol blue, 20% glycerol, 100 mM DTT, pH 6.8), samples were run on an 8% Tris/glycine gel. To ensure equal loading, 20 µg protein was loaded per well (as determined by NanoDrop) and gels were run in duplicate (one for immunoblot, and another for Coomassie staining). Protein was transferred by iBlot to a PVDF membrane, blocked in 5% skim milk-TBST (150 mM NaCl, 10 mM Tris-HCl, 0.5% Tween-20, pH 7.5) at room temperature for 1 hour, then probed with a 1:2 000 dilution of primary α-Cas9 antibody (ThermoFisher 10C11-

A12) in 5% skim milk-TBST overnight at 4°C. Following washes, the blot was probed with a 1:20 000 dilution of secondary antibody linked to alkaline phosphatase (ThermoFisher G-21060) in 5% skim milk-TBST for 1 hour at room temperature. Protein was detected by incubation with a solution of NBT/BCIP (Roche) as per the manufacturer's protocol.

RNA extraction and Reverse Transcription quantitative PCR (RT-qPCR) analysis

Cells from an overnight culture were subcultured at an OD_{600nm} of 0.01 into fresh medium with antibiotic and rhamnose, as necessary, and grown for 8 hours. Cells were harvested by centrifugation (3 minutes at 4600xg) and pellets were stored at -80°C until RNA extraction. RNA was purified and DNAse treated using the Ribopure bacteria kit (Ambion) with extended DNAse treatement (2 hours). RNA quality was verified by running on a 2% agarose gel. cDNA was synthesized with the iScript Reverse Transcriptase kit (Bio-Rad) and qPCR was performed using iQ SYBR Green mastermix (Bio-rad) on a CFX96 Touch Real-Time PCR Detection System (Bio-Rad). Primer efficiency was determined for each primer set and efficiencies between 95% and 105% were deemed acceptable. Data was analyzed using the comparative C_T method (Livak and Schmittgen, 2001; Schmittgen and Livak, 2008). Genes were normalized to a commonly used reference gene, the RNA polymerase sigma factor *sigE* (BCAM0918) (O'Grady et al., 2009; Wong et al., 2018).

Acknowledgements

This work was financially supported by grants from the Cystic Fibrosis Foundation, Cystic Fibrosis Canada, and the Natural Sciences and Engineering Research Council of Canada

(NSERC) to STC; AMH was supported by grants from the Canadian Institutes of Health Research (CIHR) and Cystic Fibrosis Canada.

The authors are grateful to Eric Déziel from the Institut National de la Recherche Scientifique – Institut Armand-Frappier for providing the miniCTX1 integration vector.

Conflict of Interest Statement

The authors declare no conflict of interest.

References

Bikard, D., Jiang, W., Samai, P., Hochschild, A., Zhang, F., and Marraffini, L.A. (2013). Programmable repression and activation of bacterial gene expression using an engineered CRISPR-Cas system. Nucleic Acids Res. *41*, 7429–7437.

Cardona, S.T., and Valvano, M.A. (2005). An expression vector containing a rhamnose-inducible promoter provides tightly regulated gene expression in *Burkholderia cenocepacia*. Plasmid *54*, 219–228.

Chapalain, A., Groleau, M.-C., Le Guillouzer, S., Miomandre, A., Vial, L., Milot, S., and Déziel, E. (2017). Interplay between 4-Hydroxy-3-Methyl-2-Alkylquinoline and N-Acyl-Homoserine Lactone Signaling in a Burkholderia cepacia Complex Clinical Strain. Front. Microbiol. *8*, 1021.

Cho, S., Choe, D., Lee, E., Kim, S.C., Palsson, B., and Cho, B.-K. (2018). High-Level dCas9 Expression Induces Abnormal Cell Morphology in Escherichia coli. ACS Synth. Biol.

689 Cho, S.W., Kim, S., Kim, J.M., and Kim, J.-S. (2013). Targeted genome engineering in
690 human cells with the Cas9 RNA-guided endonuclease. Nat. Biotechnol. *31*, 230–232.

691 Choi, K.-H., and Schweizer, H.P. (2006). mini-Tn7 insertion in bacteria with single
692 attTn7 sites: example Pseudomonas aeruginosa. Nat. Protoc. *1*, 153–161.

693 Choi, K.H., Gaynor, J.B., White, K.G., Lopez, C., Bosio, C.M., Karkhoff-Schweizer,
694 R.R., and Schweizer, H.P. (2005). A Tn7-based broad-range bacterial cloning and expression
695 system. Nat.Methods *2*, 443–448.

696 Choi, K.H., DeShazer, D., and Schweizer, H.P. (2006). mini-Tn7 insertion in bacteria
697 with multiple glmS-linked attTn7 sites: example *Burkholderia mallei* ATCC 23344. Nat. Protoc.
698 *1*, 162–169.

699 Choi, K.H., Mima, T., Casart, Y., Rholl, D., Kumar, A., Beacham, I.R., and Schweizer,
700 H.P. (2008). Genetic tools for select-agent-compliant manipulation of *Burkholderia*
701 *pseudomallei*. Appl. Environ. Microbiol. *74*, 1064–1075.

702 Choudhary, E., Thakur, P., Pareek, M., and Agarwal, N. (2015). Gene silencing by
703 CRISPR interference in mycobacteria. Nat. Commun. *6*, ncomms7267.

704 Cui, L., Vigouroux, A., Rousset, F., Varet, H., Khanna, V., and Bikard, D. (2018). A
705 CRISPRi screen in E. coli reveals sequence-specific toxicity of dCas9. Nat. Commun. *9*, 1912.

706 Datsenko, K.A., and Wanner, B.L. (2000). One-step inactivation of chromosomal genes
707 in *Escherichia coli* K-12 using PCR products. Proc Natl Acad Sci U A *97*, 6640–6645.

708 Depoorter, E., Bull, M.J., Peeters, C., Coenye, T., Vandamme, P., and Mahenthiralingam,
709 E. (2016). Burkholderia: an update on taxonomy and biotechnological potential as antibiotic
710 producers. Appl. Microbiol. Biotechnol. *100*, 5215–5229.

711 Eberl, L., and Vandamme, P. (2016). Members of the genus *Burkholderia*: good and bad
712 guys. F1000Research *5*, 1007.

713 Flannagan, R.S., Aubert, D., Kooi, C., Sokol, P.A., and Valvano, M.A. (2007).
714 Burkholderia cenocepacia requires a periplasmic HtrA protease for growth under thermal and
715 osmotic stress and for survival *in vivo*. Infect. Immun. *75*, 1679–1689.

716 Flannagan, R.S., Linn, T., and Valvano, M.A. (2008). A system for the construction of
717 targeted unmarked gene deletions in the genus *Burkholderia*. Environ. Microbiol. *10*, 1652–
718 1660.

719 Francis, N.R., Irikura, V.M., Yamaguchi, S., DeRosier, D.J., and Macnab, R.M. (1992).
720 Localization of the Salmonella typhimurium flagellar switch protein FliG to the cytoplasmic M-
721 ring face of the basal body. Proc. Natl. Acad. Sci. *89*, 6304–6308.

722 Funston, S.J., Tsaousi, K., Smyth, T.J., Twigg, M.S., Marchant, R., and Banat, I.M.
723 (2017). Enhanced rhamnolipid production in Burkholderia thailandensis transposon knockout
724 strains deficient in polyhydroxyalkanoate (PHA) synthesis. Appl. Microbiol. Biotechnol. *101*,
725 8443–8454.

726 Hoang, T.T., Kutchma, A.J., Becher, A., and Schweizer, H.P. (2000). Integration-
727 proficient plasmids for Pseudomonas aeruginosa: site-specific integration and use for
728 engineering of reporter and expression strains. Plasmid *43*, 59–72.

729 Hogan, A.M., Scoffone, V.C., Makarov, V., Gislason, A.S., Tesfu, H., Stietz, M.S.,
730 Brassinga, A.K.C., Domaratzki, M., Li, X., Azzalin, A., et al. (2018). Competitive Fitness of
731 Essential Gene Knockdowns Reveals a Broad-Spectrum Antibacterial Inhibitor of the Cell
732 Division Protein FtsZ. Antimicrob. Agents Chemother. *62*.

733 Howe, C., Sampath, A., and Spotnitz, M. (1971). The pseudomallei group: a review. J.
734 Infect. Dis. *124*, 598–606.

735 Howe, F.S., Russell, A., Lamstaes, A.R., El-Sagheer, A., Nair, A., Brown, T., and Mellor,
736 J. (2017). CRISPRi is not strand-specific at all loci and redefines the transcriptional landscape.
737 ELife *6*.

738 Jones, D.L., Leroy, P., Unoson, C., Fange, D., Ćurić, V., Lawson, M.J., and Elf, J.
739 (2017). Kinetics of dCas9 target search in Escherichia coli. Science *357*, 1420–1424.

740 Josephs, E.A., Kocak, D.D., Fitzgibbon, C.J., McMenemy, J., Gersbach, C.A., and
741 Marszalek, P.E. (2015). Structure and specificity of the RNA-guided endonuclease Cas9 during
742 DNA interrogation, target binding and cleavage. Nucleic Acids Res. *43*, 8924–8941.

743 Judson, N., and Mekalanos, J.J. (2000). TnAraOut, a transposon-based approach to
744 identify and characterize essential bacterial genes. Nat Biotechnol *18*, 740–745.

745 Kenna, D.T.D., Lilley, D., Coward, A., Martin, K., Perry, C., Pike, R., Hill, R., and
746 Turton, J.F. (2017). Prevalence of Burkholderia species, including members of Burkholderia
747 cepacia complex, among UK cystic and non-cystic fibrosis patients. J. Med. Microbiol. *66*, 490–
748 501.

749 Komatsu, H., Hayashi, F., Sasa, M., Shikata, K., Yamaguchi, S., Namba, K., and
750 Oosawa, K. (2016). Genetic analysis of revertants isolated from the rod-fragile fliF mutant of
751 Salmonella. Biophys. Physicobiology *13*, 13–25.

752 Kumar, B., and Cardona, S.T. (2016). Synthetic Cystic Fibrosis Sputum Medium
753 Regulates Flagellar Biosynthesis through the flhF Gene in *Burkholderia* cenocepacia. Front.
754 Cell. Infect. Microbiol. *6*, 65.

755 Le Guillouzer, S., Groleau, M.-C., and Déziel, E. (2017). The Complex Quorum Sensing
756 Circuitry of Burkholderia thailandensis Is Both Hierarchically and Homeostatically Organized.
757 MBio *8*.

758 Lee, H.H., Ostrov, N., Wong, B.G., Gold, M.A., Khalil, A.S., and Church, G.M. (2019).
759 Functional genomics of the rapidly replicating bacterium Vibrio natriegens by CRISPRi. Nat.
760 Microbiol.

761 Liu, X., Gallay, C., Kjos, M., Domenech, A., Slager, J., van Kessel, S.P., Knoops, K.,
762 Sorg, R.A., Zhang, J.-R., and Veening, J.-W. (2017). High-throughput CRISPRi phenotyping
763 identifies new essential genes in Streptococcus pneumoniae. Mol. Syst. Biol. *13*, 931.

764 Livak, K.J., and Schmittgen, T.D. (2001). Analysis of relative gene expression data using
765 real-time quantitative PCR and the 2(-Delta Delta C(T)) Method. Methods San Diego Calif *25*,
766 402–408.

767 Mahenthiralingam, E., Urban, T.A., and Goldberg, J.B. (2005). The multifarious,
768 multireplicon *Burkholderia cepacia* complex. Nat. Rev. Microbiol. *3*, 144–156.

769 Mao, D., Bushin, L.B., Moon, K., Wu, Y., and Seyedsayamdost, M.R. (2017). Discovery
770 of scmR as a global regulator of secondary metabolism and virulence in *Burkholderia*
771 *thailandensis* E264. Proc. Natl. Acad. Sci. U. S. A. *114*, E2920–E2928.

772 Nally, E., Groah, S.L., Pérez-Losada, M., Caldovic, L., Ljungberg, I., Chandel, N.J.,
773 Sprague, B., Hsieh, M.H., and Pohl, H.G. (2018). Identification of Burkholderia fungorum in the
774 urine of an individual with spinal cord injury and augmentation cystoplasty using 16S
775 sequencing: copathogen or innocent bystander? Spinal Cord Ser. Cases *4*, 85.

776 O'Grady, E.P., Viteri, D.F., Malott, R.J., and Sokol, P.A. (2009). Reciprocal regulation
777 by the CepIR and CciIR quorum sensing systems in *Burkholderia cenocepacia*. BMC Genomics
778 *10*.

779 Ortega, X.P., Cardona, S.T., Brown, A.R., Loutet, S.A., Flannagan, R.S., Campopiano,
780 D.J., Govan, J.R., and Valvano, M.A. (2007). A putative gene cluster for aminoarabinose
781 biosynthesis is essential for *Burkholderia cenocepacia* viability. J. Bacteriol. *189*, 3639–3644.

782 Peters, J.M., Colavin, A., Shi, H., Czarny, T.L., Larson, M.H., Wong, S., Hawkins, J.S.,
783 Lu, C.H., Koo, B.M., Marta, E., et al. (2016). A comprehensive, CRISPR-based functional
784 analysis of essential genes in bacteria. Cell *165*, 1493–1506.

785 Peters, J.M., Koo, B.-M., Patino, R., Heussler, G.E., Hearne, C.C., Qu, J., Inclan, Y.F.,
786 Hawkins, J.S., Lu, C.H.S., Silvis, M.R., et al. (2019). Enabling genetic analysis of diverse
787 bacteria with Mobile-CRISPRi. Nat. Microbiol. *4*, 244.

788 Pribytkova, T., Lightly, T.J., Kumar, B., Bernier, S.P., Sorensen, J.L., Surette, M.G., and
789 Cardona, S.T. (2014). The attenuated virulence of a Burkholderia cenocepacia paaABCDE

790 mutant is due to inhibition of quorum sensing by release of phenylacetic acid. Mol. Microbiol.
791 *94*, 522–536.

792 Qi, L.S., Larson, M.H., Gilbert, L.A., Doudna, J.A., Weissman, J.S., Arkin, A.P., and
793 Lim, W.A. (2013). Repurposing CRISPR as an RNA-guided platform for sequence-specific
794 control of gene expression. Cell *152*, 1173–1183.

795 Rhodes, K.A., and Schweizer, H.P. (2016). Antibiotic resistance in Burkholderia species.
796 Drug Resist. Updat. *28*, 82–90.

797 Rock, J.M., Hopkins, F.F., Chavez, A., Diallo, M., Chase, M.R., Gerrick, E.R., Pritchard,
798 J.R., Church, G.M., Rubin, E.J., Sassetti, C.M., et al. (2017). Programmable transcriptional
799 repression in mycobacteria using an orthogonal CRISPR interference platform. Nat. Microbiol.
800 *2*, 16274.

801 Schmittgen, T.D., and Livak, K.J. (2008). Analyzing real-time PCR data by the
802 comparative C(T) method. Nat. Protoc. *3*, 1101–1108.

803 Siegele, D.A., and Hu, J.C. (1997). Gene expression from plasmids containing the
804 araBAD promoter at subsaturating inducer concentrations represents mixed populations. Proc
805 Natl Acad Sci U A *94*, 8168–8172.

806 Tan, S.Z., Reisch, C.R., and Prather, K.L.J. (2018). A Robust CRISPRi Gene Repression
807 System inPseudomonas. J. Bacteriol. *200*, e00575-17.

808 Teufel, R., Mascaraque, V., Ismail, W., Voss, M., Perera, J., Eisenreich, W., Haehnel,
809 W., and Fuchs, G. (2010). Bacterial phenylalanine and phenylacetate catabolic pathway revealed.
810 Proc. Natl. Acad. Sci. U. S. A. *107*, 14390–14395.

811 Tomich, M., Herfst, C.A., Golden, J.W., and Mohr, C.D. (2002). Role of flagella in host
812 cell invasion by Burkholderia cepacia. Infect. Immun. *70*, 1799–1806.

813 Wong, Y.-C., Abd El Ghany, M., Ghazzali, R.N.M., Yap, S.-J., Hoh, C.-C., Pain, A., and
814 Nathan, S. (2018). Genetic Determinants Associated With *in Vivo* Survival of *Burkholderia*
815 *cenocepacia* in the *Caenorhabditis elegans* Model. Front. Microbiol. *9*, 1118.

816 Yang, P., Zhang, M., and Elsas, J.D. van (2017). Role of flagella and type four pili in the
817 co-migration of Burkholderia terrae BS001 with fungal hyphae through soil. Sci. Rep. *7*, 2997.

818

819

820